A13.11.0131

Complexation of *n* SO_2 Molecules (*n* = 1, 2, 3) with Formaldehyde and Thioformaldehyde

Luis Miguel Azofra[†, ‡] and Steve Scheiner[‡, *]

[†]Instituto de Química Médica, CSIC, Juan de la Cierva, 3, E-28006, Madrid, Spain

[‡]Department of Chemistry and Biochemistry, Utah State University, Logan, UT 84322-0300, USA

*Author to whom correspondence should be addressed.

Fax: (+1) 435-797-3390

E-mail: steve.scheiner@usu.edu

ABSTRACT

Ab initio and DFT calculations are used to examine complexes formed between H_2CO and H_2CS with 1, 2, and 3 molecules of SO_2. The nature of the interactions is probed by a variety of means, including electrostatic potentials, NBO, AIM, energy decomposition, and electron density redistribution maps. The dimers are relatively strongly bound, with interaction energies exceeding 5 kcal/mol. The structures are cyclic, containing both a O/S···S chalcogen bond and a CH···O H-bond. Addition of a second SO_2 molecule leads to a variety of heterotrimer structures, most of which resemble the original dimer, where the second SO_2 molecule engages in a chalcogen bond with the first SO_2, and a C···O attraction with the H_2CX. Some cooperativity is apparent in the trimers and tetramers, with an attractive three-body interaction energy and shortened intermolecular distances.

KEYWORDS: chalcogen bonds; CH···O hydrogen bonds; C···O bonds; SO_2–philicity; cooperativity

INTRODUCTION

The interactions between molecules represent the linchpin of our understanding of condensed phases and other aggregation phenomena. These so-called noncovalent bonds are also an essential ingredient in the structure adopted by single molecules as they control the forces between segments that are not directly bonded to one another. For example, the structure and function of biomolecular proteins are in large part controlled by noncovalent forces between amino acid residues that are not immediately adjacent to one another along the polypeptide backbone.

Of the various sorts of noncovalent interactions, the hydrogen bond (HB) is arguably the most intensively studied over the years.[1-4] The original formulation of HBs in which the proton donor and acceptor atoms are members of the very electronegative set of F, O, and N has gradually given way to a more generalized scheme which includes less electronegative atoms like Cl, S, and C.[5-8] Further, the earlier ideas that the proton acceptor atom interacts with the bridging proton via its lone electron pair has been broadened to π and σ bonds,[9-13] and even to a hydridic H atom within the context of what have come to be known as dihydrogen bonds.[11, 14-17]

Another sort of noncovalent bond arises when a pair of electronegative atoms are drawn toward one another. What would otherwise be a repulsion between atoms which both contain at least a partial negative charge becomes attractive due to the anisotropic distribution of electron density. In the case of halogen bonds, the charge distribution around a halogen atom X involved in a Y–X bond is far from spherical. There is a belt of negative charge that girdles the Y–X bond, and surrounds a crown of positive charge along the extension of the Y–X bond. The latter positively charged region is attracted to the negative charge of a neighboring molecule, commonly to an O atom, to form an attractive intermolecular X···O halogen bond.[18-23] Like HBs, the electrostatic attractions within these halogen bonds are supplemented by charge transfer from the lone pair(s) of the O atom into the σ* antibonding Y–X orbital, which tends to weaken and lengthen the latter Y–X bond. Attractive London (dispersion) forces further supplement the overall binding energy of these halogen bonds. This concept has been extended beyond halogen atoms to include other electronegative atoms, notably members of the chalcogen[24-30] and pnicogen[31-37] families, and there are very recent works that suggest that even the less electronegative C group of the periodic table can engage in very similar bonding interactions.[38, 39]

Although a great deal has been learned about the latter types of noncovalent bonds, there are a number of important remaining questions. The simple H_2CO molecule offers a number

of opportunities for study of unusual noncovalent bonds. For one thing, each C–H can act as proton donor in a nonconventional HB to a proton acceptor. The O atom can serve as HB proton acceptor, but can also participate in a chalcogen bond. The mutation of H_2CO to H_2CS presents the possibility to examine how both of these functionalities are affected when O is changed to its third-row analogue. The SO_2 molecule is especially interesting in this respect. Chalcogen bonds are in principle possible not only with the two terminal O atoms but also with the S in the center. The combination of SO_2 with H_2CO thus provides a wealth of different possible interactions, i.e., CH···O and CH···S HBs, as well as S···O and O···O chalcogen bonds. In addition, the π systems of these molecules further widen the range of possibilities wherein charge can be transferred from π orbitals and into π* antibonds.

In addition to their intrinsic and fundamental interest, formaldehyde and sulfur dioxide fill roles in industrial and environmental chemistry. Formaldehyde is emitted to the troposphere from motor vehicles and industrial emissions. The properties of this molecule in the ground state using *ab initio* studies were reviewed by Bruna *et al*.[40] Besides, Alvarez-Idaboy *et al*. and Zhao *et al*. explored the reaction between H_2CO and the radical OH.[41, 42] Sulfur dioxide is the main cause of acid rain, due to its ability to form sulfur trioxide (SO_3), which in combination with water, leads to the formation of sulfuric acid. The reaction of carbonyl oxides with SO_2 is also relevant,[43-45] due to the possible contribution of this reaction to acid rain, which was experimentally studied in the 1980s by Calvert *et al*.[46]

This work begins with the heterodimers combining SO_2 with both H_2CO and H_2CS. The entire potential energy surfaces are searched to identify all minima, and to analyze the nature of the bonding interactions which characterize each, as well as their strength. As in many such dimers, it is common to observe more than one noncovalent bond in any particular minimum-energy geometry. These arrangements permit an analysis of how each sort of bond affects the other. The ability of these sorts of noncovalent bonds to affect one another is further probed by adding a third (and fourth) molecule and analyzing the associated cooperative effects.

COMPUTATIONAL METHODS

The geometry and properties of the 1:1 and 2:1 SO_2:H_2CX (X = O, S) and also of the 3:1 SO_2:H_2CO complexes, have been studied through the use of the second-order Møller-Plesset perturbation theory (MP2)[47-50] with the aug-cc-pVDZ basis set.[51] In all cases, vibrational frequencies were calculated in order to confirm that the structures correspond to true minima and to obtain the zero point vibrational energy (ZPE). All calculations were carried out with the GAUSSIAN09 program.[52] Interaction energies were computed as the difference in energy

between the complex on one hand, and the sum of the energies of the monomers on the other, using the monomer geometries from the optimized complex. Interaction energies were corrected by the counterpoise procedure.[53] Single-point CCSD(T)[54]/aug-cc-pVTZ calculations were performed for the 1:1 complexes, using MP2/aug-cc-pVDZ geometries so as to obtain more accurate values. Also, binding energies were computed as the difference in energy between the complex on one hand, and the sum of the energies of the optimized monomers on the other, taking into account also the ZPE.

Atoms in Molecules (AIM)[55, 56] theory at MP2-level, and Natural Bond Orbital (NBO)[57] theory with the ωB97XD[58] functional, were applied to help analyze the interactions, using the AIMAll[59] and NBO3.1[60] programs. The presence of AIM bond critical points (BCP) between two centers of the monomers in the complexes,[55, 61, 62] support the presence of attractive bonding interactions, which are also quantified by NBO charge transfer between orbitals of different fragments.

Further analysis of the interaction energy by decomposition into components was carried out via DFT-SAPT calculations at the PBE0[61]/aug-cc-pVTZ level with the MOLPRO program.[63] The DFT-SAPT interaction energy, $E^{DFT\text{-}SAPT}$, is obtained as a sum of five terms (eq. 1): electrostatic (E_{ele}), exchange (E_{exc}), induction (E_{ind}), dispersion (E_{dis}) and higher-order contributions (δ_{HF}).[64]

$$E^{DFT\text{-}SAPT} = E_{ele} + E_{exc} + E_{ind} + E_{dis} + \delta_{HF} \quad (1)$$

RESULTS AND DISCUSSION

The first section below presents the molecular electrostatic potentials of the monomers, which play an instrumental role in the geometries adopted by the complexes. The succeeding sections detail the results first for the 1:1 heterodimers, followed by the 2:1 SO_2:H_2CX (X = O, S) complexes, and then the 3:1 SO_2:H_2CO heterotetramers.

Monomers

Formaldehyde (H_2CO), thioformaldehyde (H_2CS) and sulfur dioxide (SO_2) monomers adopt C_{2v} optimized geometries. The Molecular Electrostatic Potential (MEP) of each molecule is illustrated in Fig. 1, where red and blue regions correspond to negative and positive potentials, respectively. In the case of H_2CO, the two classical O lone pairs merge into one negative cloud, while there is more separation between them in H_2CS. The remainder of the surrounding region of each molecule is generally positive. The potential around the SO_2

molecule is also largely positive, but has a negative lobe on the perimeter of each O atom. In general, then, the potential of all three molecules can be characterized as generally positive, but with negative regions around oxygen atoms. The SO_2 molecule differs from the other two in that the positive region above and below the S atom extends further from the molecule. The latter positive areas represent potential binding sites for interactions with negative potentials of partner molecules. The value of the SO_2 potential at its maximum on the van der Waals (vdW) surface of the molecule lies above the S atom and amounts to 32.9 kcal/mol, consistent with the idea of a π–hole.[65]

1:1 SO_2:H_2CX (X = O, S) Heterodimers

The potential energy surface (PES) for the 1:1 SO_2:H_2CO heterodimer contains a single minimum while there are four such minima for SO_2:H_2CS. The optimized structures are gathered in Fig. 2. There is a strong similarity between the most stable complexes for both H_2CX, **A1** (SO_2:H_2CO) and **B1** (SO_2:H_2CS). Both contain what would appear to be a CH···O H-bond, as well as a bonding interaction between S of SO_2 and X. These geometries make sense from an electrostatic perspective, matching a positive region of one molecule with a negative area of its partner. The presence of specific bonding interactions are supported by AIM analysis; broken lines are introduced in Fig. 1 and succeeding molecular diagrams to indicate the presence of a BCP.

The other three SO_2:H_2CS minima **B2, B3**, and **B4** are less stable than **B1** by 3.38, 3.66 and 4.11 kcal/mol, respectively. MP2 calculations with the larger aug-cc-pVTZ basis set were performed in order to corroborate that the smaller number of minima in the 1:1 SO_2:H_2CO system is not due to a poor description at the MP2/aug-cc-pVDZ computational level. The larger basis set leaves unchanged the number and energetic ordering of the minima.

AIM analysis provides helpful information about the bond paths that link two nuclear attractors, that is, atomic centers. In the case of **A1** and **B1**, two bond paths corresponding to weak interactions are present. The first one appears between the chalcogen atom of H_2CX (O or S) and the S atom of SO_2, and a second between the O atom of SO_2 and a H atom of H_2CX (for convenience in the discussion, the interacting oxygen atom is designated O_A, and the other as O_B). Despite the general similarity of the **A1** and **B1** structures, there are certain significant differences. Compared to **A1**, the R(CH···O) distance is 0.164 Å shorter in **B1**, suggesting a stronger CH···O H-bond, and the R(S···X) distance longer by 0.430 Å. **B2** exhibits two bond paths, linking the C atom of H_2CS with both the S atom and O_A of SO_2, with interatomic distances of 3.535 and 3.071 Å, respectively. These noncovalent bonds

involving the C atom are unusual so were examined in more detail: the values of ρ at the C•••S and C•••O bond critical points are 0.0056 and 0.0071 au, respectively. These values are consistent with their characterization as bonds, as are their respective values of $\nabla^2\rho$ which are 0.0154 and 0.0251 au. In comparison, **B3** and **B4** appear to be stabilized exclusively by CH···O H-bonds.

Turning next to the interaction energies (E_{int}), Table 1 shows that **A1** and **B1** have similar counterpoise-corrected values of –4.41 and –4.32 kcal/mol in each case, raised by 1 kcal/mol in absolute terms at the CCSD(T)/aug-cc-pVTZ level. This CCSD(T) value is comparable to the experimental[66] and the more accurate theoretical[67] interaction energies within the paradigmatic H-bonded water dimer. In particular, at the same MP2/aug-cc-pVDZ level, Xantheas and Dunning Jr.'s calculations[68] yielded a value of –5.34 kcal/mol, slightly greater than the results obtained here. There is thus not much to distinguish H_2CO *vs* H_2CS with respect to its binding energy with SO_2. The other three H_2CS heterodimer structures are much less tightly bound, with $-E_{int}$ less than 2 kcal/mol. Binding energies (E_b) in Table 1 have very similar values with respect to the interaction energies, with differences less than 0.1 kcal/mol at the MP2 level. At the CCSD(T) level, these differences are still within 0.26 kcal/mol. E_{int} is consistently more negative than is E_b, as the energies of the monomers are lower in their optimized geometries,

Table 2 reports the various thermodynamic quantities for the association reactions in the 1:1 SO_2:H_2CX (X = O, S) complexes at room temperature (298 K). In all cases $\Delta S°$ is negative as is typical of such association reactions where two entities are combined into one. This negative quantity is sufficient to make $\Delta G°$ positive at 298 K despite the negative enthalpy change of this reaction. In fact, as $\Delta S°$ is less negative for the more weakly bound complexes **B3** and **B4** (i.e. less negative values of $\Delta H°$), the latter two dimers have less positive values of $\Delta G°$ than do **B1** and **B2** at 298K. This observation illustrates that the energetic disadvantage of weakly bound complexes at low T can dissipate, and even reverse, as the temperature rises in certain circumstances.

The electrostatic potential maps of Fig. 1 are consistent with, and even predictive of, the geometric configurations of the various heterodimers. As noted above, the most positive region around the SO_2 molecule lies directly above the S atom. It is this region which favorably interacts with the negative area that surrounds the O/S atoms of H_2CX in **A1** and **B1**, complemented by the attraction between the regions of opposite charge encompassed by the CH···O H-bonds. The latter electrostatic attraction is also a feature of **B3** and **B4**. Lastly,

the negative region about the O atoms of SO_2 can also interact with the positive area above the plane of the CH_2 group of H_2CS in **B2**.

It is worth comparing the interactions within these heterodimers with those of the corresponding homodimers. The potential energy surface of $(SO_2)_2$ contains three minima at the MP2/aug-cc-pVDZ computational level. The most stable structure has been previously characterized experimentally in the literature (see Scheme 1).[69] Our computed interaction energy at the CCSD(T)/aug-cc-pVTZ//MP2/aug-cc-pVDZ computational level is –3.02 kcal/mol. Fig. S1 and Table S1 of the Electronic Supplementary Information (ESI), illustrate that the PES of this homodimer contains three different minima with comparable energies. The most stable structure (**D1**) is stabilized by a S···O chalcogen bond of length 3.206 Å, and another (**D2**) by a slightly shorter O···O interaction. **D3**, somewhat less stable, is cyclic, containing a pair of S···O bonds, plus an interoxygen stabilization.

The two minima on the $(H_2CO)_2$ PES have been described in the literature with interaction energies of –4.43 and –3.58 kcal/mol at the ae-CCSD(T)/CBS computational level (see Scheme 1).[70] One structure is stabilized by a pair of CH···O H-bonds, while the other replaces one of the CH···O bonds by an apparent attraction between C and O. $(H_2CS)_2$ seems to be an unstable structure which leads to the dimerization of the monomers through the formation of a formal S–C covalent bond as has been described recently by Krantz et al. in the literature[71] (see Scheme 1). Overall, then, the interaction energies of these various homodimers are somewhat smaller than the same quantities in the heterodimers.

Scheme 1. $(H_2CO)_2$ (*a*, *b*) and $(SO_2)_2$ (*c*) dimers, and $(H_2CS)_2$ molecule described in the literature. See ref.[69], ref.[70] and ref.[71], respectively.

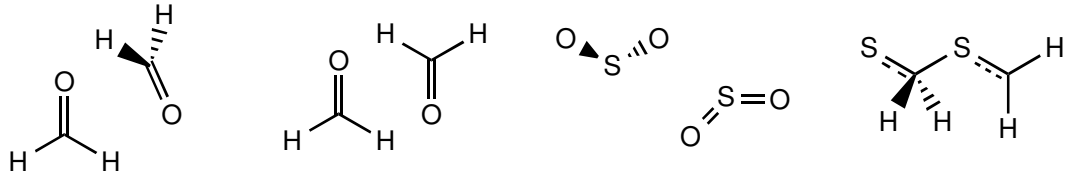

(*a*, C_s) (*b*, C_{2h}) (*c*, C_s) (*d*, C_1)

NBO analysis offers useful insights into the fundamental nature of the intermolecular forces, dealing primarily with charge-transfer interactions between particular molecular orbitals. Table 3 lists the main intermolecular second-order perturbation energies, $E(2)$ for the 1:1 SO_2:H_2CX (X = O, S) complexes (a visual depiction of the involved orbitals is contained in the ESI as Fig. S2). The primary component for the **A1** and **B1** structures may be seen to

be transfer from a lone pair of the O/S atom of H_2CX into a S–O_B π* antibonding orbital of SO_2. Both structures are stabilized also by several smaller auxiliary interactions, most notably from O lone pairs of SO_2 to a σ* antibonding CH orbital of H_2CX (there are two such interactions in each case, one for each O lone pair, summed together in Table 3). The latter transfer is consistent with the notion of a CH···O H-bond in these heterodimers, buttressed by the short R(H···O) distances of 2.412 and 2.248 Å, respectively. The shorter H-bond length in the H_2CS complex is consistent with the larger combined $E(2)$ values of 3.75 kcal/mol, compared to 1.78 kcal/mol for **A1**. The latter **A1** dimer is also stabilized by a transfer from the H_2CO O atom into the S–O_A σ* antibonding orbital of SO_2, amounting to 0.55 kcal/mol.

The less stable **B2** complex appears to contain a single noncovalent bond, involving transfer from an O_A lone pair of SO_2 into a π* antibonding C–S orbital of H_2CS (1.25 kcal/mol). This NBO picture contrasts with the AIM interpretation in Fig. 2 that would suggest C···S and C···O bonds. Examination of the electrostatic potentials in Fig. 1 would not lead to the characterization of this interaction as involving a so-called π–hole above the C atom of H_2CS. The $O_{lp}\rightarrow\pi^*$(C=S) transfer is reminiscent of similar $O_{lp}\rightarrow\pi^*$(C=O) interactions suggested by the Raines' group to help stabilize certain polypeptide structures.[72, 73] There are no $E(2)$ values in structures **B3** or **B4** that reach the 0.5 kcal/mol threshold, so one might suppose that any CH···O bonds are rather weak, consistent with their lengths in excess of 2.7 Å. Indeed, one might consider the less stable structures in Fig. 2 to be primarily bound together by favorable Coulombic interactions between the MEPs of the two monomers (see Fig. 1).

Another useful window into the nature of the interaction arises from a decomposition of the total interaction energy into individual components. This partitioning was carried out via the DFT-SAPT methodology (PBE0/aug-cc-pVTZ), and the components are displayed in Table 4. The DFT-SAPT analysis used the experimental ionization potentials, in eV, for H_2CO (10.88)[74] H_2CS (9.376 ± 0.003)[75] and SO_2 (12.5 ± 0.1),[76] from NIST.[77] It is first clear that the largest attractive component is the electrostatic energy which is in absolute terms more than 9 kcal/mol for **A1** and **B1**, followed by dispersion which is roughly half that amount. Somewhat smaller is δ_{HF} which represents higher-order effects. Induction makes the smallest contribution to the attraction. All of these terms suffer a substantial reduction in the other complexes, **B2**-**B4**, consistent with their overall weaker nature. It might be worth noting, however, that in the latter three dimers, the dispersion energy is essentially equal to the electrostatic attraction.

As two molecules begin to interact with one another, they perturb one another's electron clouds. The shifts in total electron density that occur as a result of the formation of each complex are illustrated in Fig. 3, where purple and yellow regions indicate respectively gains and losses of density, relative to the isolated monomers. A common value of ±0.001 au was used in diagrams for **A1** and **B1**. The shifts in these two structures show very similar patterns. The CH···O HBs in the lower part of each dimer are verified by the characteristic loss of density around the bridging H, and the buildup in the lone pair region of the proton-acceptor O atom. The O···X chalcogen bond in the upper portion of each molecule is represented by a loss in the lone pair region of the SO_2 molecule's O atom, and gain to the left of the X atom of H_2CX. Density shifts in the other heterodimers are much smaller, and are barely evident with the use of the common ±0.001 au contour, so are displayed in Fig. 3 using a smaller contour value of ±0.0005 au. The patterns in **B3** and **B4** are consistent with the usual fingerprint of HBs: loss around the bridging proton and gain by the proton-acceptor atom. **B2** does not fit this pattern, instead showing a gain around the O atom of SO_2, and the S of H_2CS, coupled with loss in the region of the CH_2 moiety.

2:1 SO_2:CH_2X (X = O, S) Heterotrimers

The PES of 2:1 SO_2:H_2CX (X = O, S) mixed heterotrimers were searched following a dual strategy: i) inserting a second SO_2 molecule in various locations around the aforementioned 1:1 complexes; and ii) fresh starting points, with no prejudice toward the 1:1 structures.

Fig. 4 gathers together the minima obtained for the 2:1 complexes between SO_2 and H_2CO at the MP2/aug-cc-pVDZ computational level, all of which are in some sense derived from the **A1** dimer, in that one SO_2 molecule is connected to H_2CO by both a CH···O HB and a S···O chalcogen bond. The total of 11 minima (**A1a** to **A1k**) can be classified into three main groups:

i) **A1a**-**A1e** are cyclic structures in that the second SO_2 molecule engages in a chalcogen bond with the first SO_2, and a C···O attraction with the H_2CO.

ii) **A1h** and **A1i** are also cyclic, and the second SO_2 is bound by S···O chalcogen bonds alone.

iii) **A1f**, **A1g, A1j**, **A1k** are all noncyclic, that is, linear, in that there are two end molecules that have no interaction with one another. The H_2CO molecule is centrally disposed between two SO_2 units in **A1f**, **A1g,** and **Aik**, while it is a SO_2 molecule in the center of **A1j**. **A1f** and **A1g** are similar in that both are of C_s symmetry and contain a pair of symmetrically equivalent S···O chalcogen bonds, and a pair of CH···O H-bonds; **A1k** forgoes one of the two S···O bonds.

The interaction energies and the pairwise energies derived from multi-body analysis of these heterotrimers are reported in Table 5. As might be noted from the last column, group (i) **A1a**-**A1e** is most stable, all within 0.64 kcal/mol of one another, with **A1a** and **A1b** particularly close. Next in energy are two of the linear complexes, **A1f** and **A1g**, followed by group (ii) whose energies exceed that of the global minimum **A1b** by more than 1 kcal/mol. Least stable of all are the two cyclic complexes **A1j** and **A1k**.

Examination of the pairwise interaction energies reveals some interesting patterns. First, with respect to group (i) **A1a**-**A1e**, there is one particularly large pairwise interaction of roughly 6 kcal/mol, and two smaller ones of 2-3 kcal/mol in absolute terms. They all show evidence of positive cooperativity, with a three-body Δ^3E term of about –1 kcal/mol (negative, i.e., attractive values of Δ^3E, correspond to positive cooperativity). This cooperativity is consistent with the observation that each of the three molecules plays the role of simultaneous electron donor and acceptor. Not surprisingly, the noncyclic trimers all have at least one pairwise interaction energy between end molecules that is very small, ±0.1 kcal/mol or less. The cooperativity is small and negative (positive Δ^3E) for **A1f** and **A1g** since the second SO_2 molecule makes the O of the central H_2CO a double proton donor, and both H atoms of H_2CO an acceptor. The same small negative cooperativity is evident in group (ii) **A1h** and **A1i** as the new SO_2 molecule attempts to form a second chalcogen bond with the same H_2CO O atom, as well as a second S···O bond with the first SO_2 molecule. In all cases, the energy associated with the monomer's deformation within the complex (E_r) is less than 1 kcal/mol, so is not a major factor.

It might be noted that E_{12}, the interaction energy between the first SO_2 molecule and H_2CO in the 2:1 complexes tends to be slightly less negative than the same quantity within the **A1** dimer (–6.01 kcal/mol). This small reduction is likely the consequence of the deviation of the intermolecular geometry in the trimer vis a vis the optimized dimer. More specifically, the R(S···O) distance in dimer **A1** is 2.768 Å, and is shortened to the 2.669-2.690 Å range in **A1a**-**A1e**, where the cooperativity is positive, but lengthened to 2.816 and 2.827 Å in **A1f** and **A1g**, respectively, where negative cooperativity is apparent in Table 5. The pattern in R(H···O) for the CH···O H-bond is not as dramatic, undergoing only small changes upon trimerization.

In addition to structures **A1a**-**A1k**, two more minima were identified on the surface of this heterotrimer that could not be readily identified as simple additions to **A1**. Neither **A2a** nor **A3a** (see Fig. S3 and Table S2 of the ESI) contain a CH···O HB and a S···O chalcogen

bond between H_2CO and a single SO_2 molecule. Both trimers are of fairly high energy, so not likely to be observed. Both are c

As reported in Table 3, the primary NBO charge transfer of the **A1** dimer arose from the H_2CO O lone pairs to the π^* SO_B antibonding orbital of SO_2, with a value of $E(2)$ equal to 8.67 kcal/mol. This interaction was supplemented by a CH···O HB, with $E(2)$ equal to 1.78 kcal/mol for $O_{Alp} \rightarrow \sigma^*(CH)$. Similar $E(2)$ quantities reported in Table S3 of the ESI, indicate that these interactions persist in the **A1**-type heterotrimers **A1a-A1k**, but generally at a reduced magnitude. Taking **A1a** as an example, the $O_{lp} \rightarrow \pi^*(OS)$ $E(2)$ is 5.21 kcal/mol, and the $O_{lp} \rightarrow \sigma^*(CH)$ H-bonding quantity 0.70 kcal/mol (although the latter is augmented by a $\pi(OS) \rightarrow \sigma^*(CH)$ transfer of 0.87 kcal/mol). The chief NBO interaction identified for the second SO_2 molecule arises from the transfer from its O lone pair to the $\pi^*(CO)$ antibonding orbital of H_2CO, with $E(2)$ = 1.03 kcal/mol. The total of all three of these quantities, along with an $O_{lp} \rightarrow \sigma^*(OS)$ $E(2)$ of 1.32 kcal/mol, is 9.04 kcal/mol, which is less than the total $E(2)$ of 11.69 kcal/mol in the **A1** dimer. Hence one can say that the positive cooperativity of **A1a** is not accurately reflected as a simple sum of the $E(2)$ quantities.

A1c and **A1d**, on the other hand, suffer only a very small diminution of these quantities. The value of $O_{lp} \rightarrow \pi^*(OS)$ $E(2)$ is 8.13 and 7.81 kcal/mol for **A1c** and **A1d**, respectively. This term is quite a bit smaller in **A1e**, the last member of trimer group (i), as well as in members of group (ii), **A1h** and **A1i**. Turning next to the linear members of group (iii), $E(2)$ for this interaction amounts to 6.05 and 5.93 kcal/mol for **A1f** and **A1g** respectively, consistent with the participation of the central H_2CO molecule as double electron donor, and the positive value of Δ^3E in Table 5. This same quantity is considerably larger for **A1j** and **A1k**, rising to 10.07 kcal/mol for the latter. Note that Δ^3E is negative for both of these structures, consistent with large values of $E(2)$.

Fig. 5 gathers the structures of the S-analogue 2:1 SO_2:H_2CS heterotrimers that were located on the PES. These structures can all be considered as derivative of the **B1** dimer in that they contain both S···S and CH···O attractions; those resembling **B2**, **B3** and **B4** were of much higher energy. The total interaction energies of these trimers are presented in the last column of Table 6, along with a multi-body analysis. The pairwise values of E_{12} in Table 6 are all fairly similar to the same quantity of –6.09 kcal/mol in the **B1** dimer. Again, some of these geometries can be categorized as cyclic, and the remaining three **B1e**, **B1f**, and **B1h** as linear.

In the three lowest energy structures, the second SO_2 molecule engages in a C···O bond with H_2CS according to AIM analysis, complemented by S···O bonds; the third SO_2 molecule is bound by three separate S···O bonds in **B1d**. It may be noted that these four minima all exhibit relatively high degrees of cooperativity, viz. negative values of Δ^3E in Table 6. Linear trimers **B1e** and **B1f** are quite similar to one another, with a pair of CH···O H-bonds, combined with a pair of S···S chalcogen bonds. As the central molecule must fulfill the role of double proton donor as well as double S···S electron acceptor, it is not surprising to note positive Δ^3E quantities in Table 6. Such negative cooperativity is also in evidence in **B1g**, probably due to the fact that the central SO_2 molecule is engaged as multiple electron donor in a pair of S···O bonds.

Another measure of cooperativity emerges from comparisons of intermolecular distances. The R(S···S) distance in **B1** is 3.198 Å, and the CH···O bond distance is 2.248 Å. The former distance contracts to less than the overall 3.067 Å in trimers **B1a-B1d**, and the H-bond is also shortened. In contrast, R(S···S) is elongated to 3.263 and 3.267 Å in linear trimers **B1e** and **B1f**, respectively.

In addition to those structures in Fig. 5 that are derived from **B1**, two other minima were located. **B5a** and **B5b**, lie 2.12 and 3.03 kcal/mol, respectively, above the global minimum **B1a** (see Fig. S5 and Table S4 of the ESI). **B5a** is topologically similar to **A2a**, with similar bonding patterns. Likewise, one can see strong similarities between the following pairs: **B1a/A1a, B1c/A1c, B1e/A1f, B1f/A1g** and **B1h/A1j**.

As may be noted in the molecular diagrams, a number of complexes contain what is characterized as a C···O bond in terms of an AIM bond critical point. Such C···O bonds are present, for example, in the most stable minima of 2:1 SO_2:CH_2X (X = O, S) heterotrimers. This interaction takes a different form within the framework of interorbital interactions that are analyzed via NBO. Taking **A1a** as an example, AIM situates a C···O bond between the C of H_2CO and an O atom of the second SO_2 molecule with an interatomic R(C···O) distance of 2.820 Å (see Fig. 4). NBO, on the other hand, indicates a charge transfer, with $E(2)$ = 1.03 kcal/mol, from the lone pairs of this O atom of SO_2 into a π* antibonding CO orbital of H_2CO. And indeed, comparison of AIM and NBO data confirms the commonality that such a C···O bond critical point appears as a NBO $O_{lp}\rightarrow\pi^*$(CO) charge transfer.

3:1 SO_2:H_2CO Heterotetramers

An exhaustive search of the potential energy surface of the 3:1 complexes between SO_2 and H_2CO yielded 40 minima (**C1**-**C40**). As may be noted in Fig. S6, all are related to dimer **A1** in the disposition of H_2CO and one of the SO_2 molecules. These structures span an energy

range of 5.12 kcal/mol, with total interaction energies between –19.78 and –14.66 kcal/mol. Examination of Table S5 reveals that the cooperativity effects are minimal at the four-body level, with $\Delta^4 E$ less than 0.17 kcal/mol. Three-body effects are much larger, with positive cooperativity amounting to $-\Delta^3 E$ larger than 2 kcal/mol in some configurations (up to 2.55 kcal/mol), considerably greater than in the trimers. It is tempting to speculate that this cooperativity will continue to grow as the system approaches the situation approximating a single H_2CO molecule in SO_2 solvent.

SUMMARY AND CONCLUSIONS

SO_2 forms rather strongly bound complexes with both H_2CO and H_2CS, with interaction energies slightly greater than 5 kcal/mol. These heterodimers are held together by a pair of attractive interactions comprising a O/S···S chalcogen bond and a CH···O H-bond. The former interaction is verified both by an AIM bond critical point, and NBO charge transfer from the O/S lone pair to the S–O π* antibonding orbital. There are additional, less stable, dimers on the SO_2:H_2CS surface, which are based on weak CH···O H-bonds alone, or on a small degree of charge transfer from a SO_2 oxygen lone pair to the C–S π* antibonding orbital of H_2CS. In all cases, the minima on either surface are fully consistent with favorable interactions between the electrostatic potentials of the pair of monomers.

When a second SO_2 molecule is added to form the 2:1 SO_2:H_2CO heterotrimers, the most stable structure is cyclic, wherein the second SO_2 molecule engages in a chalcogen bond with the first SO_2, and a C···O attraction with the H_2CO. The latter is associated with transfer from the O lone pair to the π*(CO) antibonding orbital of H_2CO. Other minima of the total of 13 identified are varied, some of which are noncyclic, but most retain the basic original dimer structure. There is a certain degree of positive cooperativity in these trimers, characterized both by contractions of intermolecular distances and a three-body interaction energy in excess of 1 kcal/mol in absolute terms. Similar findings pertain to the 2:1 SO_2:H_2CS heterotrimer S-analogues.

Addition of a third SO_2 molecule leads to a large number of 2:1 SO_2:H_2CO heterotetramers, 40 to be exact. Like the trimers, they retain the basic dimer geometry, characterized by a S···O chalcogen bond and a CH···O H-bond. The total interaction energies of these tetramers range between –20 and –15 kcal/mol. Although only minimal four-body interactions are observed, the sum of three-body terms rises above –2 kcal/mol.

SUPPLEMENTARY MATERIAL

Electronic Supplementary Information (ESI) associated with this article can be found via Internet at http://aip.org/. In addition to the tables and figures, also contained is a complete annex with the molecular graphs of the most important complexes.

ACKNOWLEDGMENTS

LMA thanks the MICINN for a PhD grant (No. BES–2010–031225), the MINECO (Project No. CTQ2012–35513–C02–02) and the Comunidad Autónoma de Madrid (Project MADRISOLAR2, ref. S2009/PPQ–1533) for continuing support. Financial support from NSF is acknowledged (CHE-1026826). Computer, storage and other resources from the Division of Research Computing in the Office of Research and Graduate Studies at Utah State University and the CTI (CSIC) are gratefully acknowledged.

REFERENCES

1. P. Schuster, G. Zundel and C. Sandorfy, The Hydrogen Bond (North-Holland Publishing Co., Amsterdam, The Netherlands, 1976).
2. S. Scheiner, Hydrogen Bonding: A Theoretical Perspective (Oxford University Press, New York, USA, 1997).
3. S. J. Grabowski, Challenges and Advances in Computational Chemistry and Physics, edited by J. Leszczynski (Springer, Dordrecht, The Netherlands, 2006).
4. G. Gilli and P. Gilli, The Nature of the Hydrogen Bond (Oxford University Press, Oxford, UK, 2009).
5. A. Bhattacherjee, Y. Matsuda, A. Fujii and S. Wategaonkar, ChemPhysChem **14**, 905 (2013).
6. K. Grzechnik, K. Rutkowski and Z. Mielke, J. Mol. Struct.: THEOCHEM **1009**, 96 (2012).
7. H. S. Biswal and S. Wategaonkar, J. Phys. Chem. A **113**, 12774 (2009).
8. E. Arunan, G. R. Desiraju, R. A. Klein, J. Sadlej, S. Scheiner, I. Alkorta, D. C. Clary, R. H. Crabtree, J. J. Dannenberg, P. Hobza, H. G. Kjaergaard, A. C. Legon, B. Mennucci and D. J. Nesbitt, Pure Appl. Chem. **83**, 1637 (2011).
9. M. Saggu, N. M. Levinson and S. G. Boxer, J. Am. Chem. Soc. **134**, 18986 (2012).
10. M. Nishio, PCCP **13**, 13873 (2011).
11. B. G. d. Oliveira, PCCP **15**, 37 (2013).
12. O. Takahashi, Y. Kohno and M. Nishio, Chem. Rev. **110**, 6049 (2010).
13. T. Nakanaga, K. Buchhold and F. Ito, Chem. Phys. **288**, 69 (2003).
14. T. Kar and S. Scheiner, J. Chem. Phys. **119**, 1473 (2003).
15. P. C. Singh and G. N. Patwari, Chem. Phys. Lett. **419**, 265 (2006).
16. N. V. Belkova, E. S. Shubina and L. M. Epstein, Acc. Chem. Res. **38**, 624 (2005).
17. M. Solimannejad and S. Scheiner, J. Phys. Chem. A **109**, 11933 (2005).
18. J. P. M. Lommerse, A. J. Stone, R. Taylor and F. H. Allen, J. Am. Chem. Soc. **118**, 3108 (1996).
19. P. Metrangolo and G. Resnati, Science **321**, 918 (2008).
20. P. Politzer, J. S. Murray and M. Concha, J. Mol. Model. **14**, 659 (2008).
21. P. Hobza and K. Muller-Dethlefs, Non-Covalent Interactions (RSC, Cambridge, UK, 2010).
22. W. Zierkiewicz, D. Michalska and T. Zeegers-Huyskens, PCCP **12**, 13681 (2010).
23. U. Adhikari and S. Scheiner, Chem. Phys. Lett. **532**, 31 (2012).
24. R. E. Rosenfield, R. Parthasarathy and J. D. Dunitz, J. Am. Chem. Soc. **99**, 4860 (1977).
25. F. T. Burling and B. M. Goldstein, J. Am. Chem. Soc. **114**, 2313 (1992).
26. D. B. Werz, R. Gleiter and F. Rominger, J. Am. Chem. Soc. **124**, 10638 (2002).
27. M. Iwaoka, S. Takemoto and S. Tomoda, J. Am. Chem. Soc. **124**, 10613 (2002).
28. C. Bleiholder, D. B. Werz, H. Koppel and R. Gleiter, J. Am. Chem. Soc. **128**, 2666 (2006).
29. G. Sánchez-Sanz, I. Alkorta and J. Elguero, Mol. Phys. **109**, 2543 (2011).
30. M. Jablonski, J. Phys. Chem. A **116**, 3753 (2012).
31. R. D. Chapman, R. D. Gilardi, M. F. Welker and C. B. Kreutzberger, J. Org. Chem. **64**, 960 (1999).
32. G. Muller, J. Brand and S. E. Jetter, Zeitschrift Naturforschung, B: Chem. Sci. **56**, 1163 (2001).
33. U. Adhikari and S. Scheiner, Chem. Phys. Lett. **536**, 30 (2012).
34. S. Tschirschwitz, P. Lönnecke and E. Hey-Hawkins, Dalton Trans. **2007**, 1377 (2007).

35. S. Scheiner, J. Phys. Chem. A **115**, 11202 (2011).
36. M. Bühl, P. Kilian and J. D. Woollins, ChemPhysChem **12**, 2405 (2011).
37. S. Scheiner, Acc. Chem. Res. **46**, 280 (2013).
38. A. Bauzá, T. J. Mooibroek and A. Frontera, Angew. Chem. Int. Ed. **52**, 12317 (2013).
39. D. Mani and E. Arunan, PCCP, **15**, 14377 (2013)
40. P. J. Bruna, M. R. J. Hachey and F. Grein, J. Mol. Struct.: THEOCHEM **400**, 177 (1997).
41. J. Raúl Alvarez-Idaboy, N. Mora-Diez, R. J. Boyd and A. Vivier-Bunge, J. Am. Chem. Soc. **123**, 2018 (2001).
42. Z. Jiao, P. Luo, Y. Wu, S. Ding and Z. Zhang, J. Hazard. Mater. **134**, 176 (2006).
43. P. Aplincourt and M. F. Ruiz-López, J. Am. Chem. Soc. **122**, 8990 (2000).
44. S. Hatakeyama, H. Kobayashi, Z. Y. Lin, H. Takagi and H. Akimoto, J. Phys. Chem. **90**, 4131 (1986).
45. T. W. Ebbesen, J. Phys. Chem. **88**, 4131 (1984).
46. J. G. Calvert, A. Lazrus, G. L. Kok, B. G. Heikes, J. G. Walega, J. Lind and C. A. Cantrell, Nature **317**, 27 (1985).
47. C. Møller and M. S. Plesset, Phys. Rev. **46**, 618 (1934).
48. J. A. Pople, J. S. Binkley and R. Seeger, Int. J. Quantum Chem. **10**, 1 (1976).
49. J. A. Pople, R. Seeger and R. Krishnan, Int. J. Quantum Chem. **12**, 149 (1977).
50. R. Krishnan and J. A. Pople, Int. J. Quantum Chem. **14**, 91 (1978).
51. J. E. Del Bene, J. Phys. Chem. **97**, 107 (1993).
52. M. J. Frisch, G. W. Trucks, H. B. Schlegel, G. E. Scuseria, M. A. Robb, J. R. Cheeseman, G. Scalmani, V. Barone, B. Mennucci, G. A. Petersson, H. Nakatsuji, M. Caricato, X. Li, H. P. Hratchian, A. F. Izmaylov, J. Bloino, G. Zheng, J. L. Sonnenberg, M. Hada, M. Ehara, K. Toyota, R. Fukuda, J. Hasegawa, M. Ishida, T. Nakajima, Y. Honda, O. Kitao, H. Nakai, T. Vreven, J. Montgomery, J. A., J. E. Peralta, F. Ogliaro, M. Bearpark, J. J. Heyd, E. Brothers, K. N. Kudin, V. N. Staroverov, R. Kobayashi, J. Normand, K. Raghavachari, A. Rendell, J. C. Burant, S. S. Iyengar, J. Tomasi, M. Cossi, N. Rega, N. J. Millam, M. Klene, J. E. Knox, J. B. Cross, V. Bakken, C. Adamo, J. Jaramillo, R. Gomperts, R. E. Stratmann, O. Yazyev, A. J. Austin, R. Cammi, C. Pomelli, J. W. Ochterski, R. L. Martin, K. Morokuma, V. G. Zakrzewski, G. A. Voth, P. Salvador, J. J. Dannenberg, S. Dapprich, A. D. Daniels, Ö. Farkas, J. B. Foresman, J. V. Ortiz, J. Cioslowski and D. J. Fox, (Gaussian Inc., Wallingford CT, 2009).
53. S. F. Boys and F. Bernardi, Mol. Phys. **19**, 553 (1970).
54. J. A. Pople, M. Head-Gordon and K. Raghavachari, J. Chem. Phys. **87**, 5968 (1987).
55. R. F. W. Bader, Atoms in Molecules: A Quantum Theory (Clarendon Press, Oxford, UK, 1990).
56. P. L. A. Popelier, Atoms In Molecules. An introduction (Prentice Hall, Harlow, UK, 2000).
57. F. Weinhold and C. R. Landis, Valency and Bonding. A Natural Bond Orbital Donor-Aceptor Perspective (Cambridge Press, Cambridge, UK, 2005).
58. J.-D. Chai and M. Head-Gordon, PCCP **10**, 6615 (2008).
59. T. A. Keith, TK Gristmill Software, Overland Park KS, USA, 2013.
60. E. D. Glendening, J. K. Badenhoop, A. E. Reed, J. E. Carpenter, J. A. Bohmann, C. M. Morales, C. R. Landis and F. Weinhold, Theoretical Chemistry Institute, University of Wisconsin, Madison, USA.
61. I. Rozas, I. Alkorta and J. Elguero, J. Am. Chem. Soc. **122**, 11154 (2000).
62. D. Cremer, Croat. Chem. Acta **57**, 1259 (1984).

63. H.-J. Werner, P. J. Knowles, F. R. Manby, M. Schütz, P. Celani, G. Knizia, T. Korona, R. Lindh, A. Mitrushenkov, G. Rauhut, T. B. Adler, R. D. Amos, A. Bernhardsson, A. Berning, D. L. Cooper, M. J. O. Deegan, A. J. Dobbyn, F. Eckert, E. Goll, C. Hampel, A. Hesselmann, G. Hetzer, T. Hrenar, G. Jansen, C. Köppl, Y. Liu, A. W. Lloyd, R. A. Mata, A. J. May, S. J. McNicholas, W. Meyer, M. E. Mura, A. Nicklaß, P. Palmieri, K. Pflüger, R. Pitzer, M. Reiher, T. Shiozaki, H. Stoll, A. J. Stone, R. Tarroni, T. Thorsteinsson, M. Wang and A. Wolf, 2012
64. G. Chałasiński and M. M. Szcześniak, Chem. Rev. **100**, 4227 (2000).
65. J. Murray, P. Lane, T. Clark, K. Riley and P. Politzer, J. Mol. Model. **18**, 541 (2012).
66. J. Reimers, R. Watts and M. Klein, Chem. Phys. **64**, 95 (1982).
67. J. R. Lane, J. Chem. Theory Comput. **9**, 316 (2012).
68. S. S. Xantheas and T. H. Dunning, J. Chem. Phys. **99**, 8774 (1993).
69. D. D. Nelson, G. T. Fraser and W. Klemperer, J. Chem. Phys. **83**, 945 (1985).
70. G. A. Dolgonos, Chem. Phys. Lett. **585**, 37 (2013).
71. K. E. Krantz, A. Senning and I. Shim, J. Mol. Struct.: THEOCHEM **944**, 83 (2010).
72. C. E. Jakobsche, A. Choudhary, S. J. Miller and R. T. Raines, J. Am. Chem. Soc. **132**, 6651 (2010).
73. G. J. Bartlett, R. W. Newberry, B. VanVeller, R. T. Raines and D. N. Woolfson, J. Am. Chem. Soc. **135**, 18682 (2013).
74. K. Ohno, K. Okamura, H. Yamakado, S. Hoshino, T. Takami and M. Yamauchi, J. Phys. Chem. **99**, 14247 (1995).
75. B. Ruscic and J. Berkowitz, J. Chem. Phys. **98**, 2568 (1993).
76. K. B. Snow and T. F. Thomas, Int. J. Mass Spectrom. Ion Processes **96**, 49 (1990).
77. NIST-Chemistry-Webbook, http://webbook.nist.gov/chemistry/

Table 1. Interaction E_{int} and binding E_b energies (kcal/mol) for the 1:1 SO_2:H_2CX (X = O, S) complexes at MP2/aug-cc-pVDZ and at CCSD(T)/aug-cc-pVTZ (single point) computational levels.

	MP2		CCSD(T)	
Complex	E_{int} (CC)[a]	E_b (ZPE)[b]	E_{int} (CC)[a]	E_b
A1	–6.01 (–4.41)	–5.93 (–4.54)	–6.15 (–5.42)	–6.08
B1	–6.09 (–4.32)	–6.02 (–4.73)	–6.05 (–5.25)	–5.79
B2	–2.65 (–1.50)	–2.64 (–2.08)	–2.20 (–1.70)	–2.12
B3	–2.37 (–1.42)	–2.36 (–1.90)	–2.25 (–1.76)	–2.19
B4	–1.91 (–1.21)	–1.91 (–1.59)	–1.77 (–1.39)	–1.78

[a]Counterpoise corrections to basis set superposition error (BSSE) added in parentheses.
[b]Zero point vibrational energy (ZPE) added in parentheses.

Table 2. Entropy, enthalpy and Gibbs free energies for the association reactions of the 1:1 SO_2:H_2CX (X = O, S) complexes at the MP2/aug-cc-pVDZ computational level at room temperature (298 K).

Complex	ΔS°, cal mol^{-1} K^{-1}	ΔH°, kcal mol^{-1}	ΔG°, kcal mol^{-1}
A1	–27.22	–4.45	3.67
B1	–27.86	–4.62	3.68
B2	–18.39	–1.40	4.08
B3	–14.65	–1.11	3.25
B4	–9.05	–0.69	2.01

Table 3. Second-order perturbation NBO energy, $E(2)$ (kcal/mol) for the 1:1 SO_2:H_2CX (X = O, S) complexes at ωB97XD/aug-cc-pVDZ computational level for intermolecular donor/acceptor interactions.

Complex	Donor/Acceptor	Type	$E(2)$
A1	H_2CO/SO_2	$O_{lp}\rightarrow\pi^*(O_BS)$	8.67
	H_2CO/SO_2	$O_{lp}\rightarrow\pi^*(O_BS)$	0.69
	H_2CO/SO_2	$O_{lp}\rightarrow\sigma^*(O_AS)$	0.55
	SO_2/H_2CO	$O_{Alp}\rightarrow\sigma^*(CH)$	1.78
B1	H_2CS/SO_2	$S_{lp}\rightarrow\pi^*(O_BS)$	11.84
	SO_2/H_2CS	$O_{Alp}\rightarrow\sigma^*(CH)$	3.75
B2	SO_2/H_2CS	$O_{Alp}\rightarrow\pi^*(CS)$	1.25

Table 4. Interaction energy components (kcal/mol) for the 1:1 SO_2:H_2CX (X = O, S) complexes, calculated using the DFT-SAPT (PBE0/aug-cc-pVTZ) methodology.

Complex	E_{ele}	E_{exc}	E_{ind}	E_{dis}	δ_{HF}	$E^{DFT\text{-}SAPT}$
A1	–9.17	12.21	–1.67	–4.80	–2.25	–5.68
B1	–9.22	14.38	–1.82	–5.80	–3.85	–6.31
B2	–2.67	4.25	–0.31	–2.82	–0.43	–1.98
B3	–1.91	2.33	–0.14	–1.96	–0.14	–1.82
B4	–1.36	1.58	–0.12	–1.39	–0.10	–1.39

Table 5. Multi-body analysis (kcal/mol) for the 2:1 SO_2:H_2CO complexes derived from **A1** at the MP2/aug-cc-pVDZ computational level. Subscripts 1, 2 and 3 in the coupled energy terms, refer to H_2CO, derived SO_2 molecule from **A1** and the second SO_2 molecule, respectively.

Complex	E_{12}	E_{13}	E_{23}	$\Sigma\Delta^2E$	Δ^3E	total E_{int}
A1a	–5.84	–2.41	–2.99	–11.24	–1.14	–12.38
A1b	–5.88	–2.47	–2.93	–11.28	–1.12	–12.40
A1c	–5.80	–1.94	–3.26	–11.00	–1.29	–12.29
A1d	–5.88	–1.74	–3.42	–11.04	–0.94	–11.98
A1e	–5.85	–2.00	–2.73	–10.58	–1.16	–11.74
A1f	–6.00	–6.00	–0.06	–12.06	0.38	–11.68
A1g	–6.00	–6.00	0.10	–11.90	0.41	–11.49
A1h	–5.82	–3.10	–2.46	–11.38	0.23	–11.15
A1i	–5.88	–3.37	–1.73	–10.99	0.08	–10.91
A1j	–6.05	0.00	–3.76	–9.81	–0.17	–9.98
A1k	–6.01	–1.65	–0.10	–7.76	–0.37	–8.13

Table 6. Multi-body analysis (kcal/mol) for the 2:1 SO_2:H_2CS complexes derived from **B1** at MP2/aug-cc-pVDZ computational level. Subscripts 1, 2 and 3 in the coupled energy terms, refer to H_2CO, derived SO_2 molecule from **B1** and the second SO_2 molecule, respectively.

Complex	E_{12}	E_{13}	E_{23}	$\Sigma\Delta^2E$	Δ^3E	total E_{int}
B1a	–5.94	–2.52	–2.81	–11.27	–1.44	–12.71
B1b	–5.89	–1.99	–3.29	–11.17	–1.24	–12.41
B1c	–5.98	–1.67	–3.27	–10.92	–1.38	–12.30
B1d	–5.97	–1.56	–3.18	–10.71	–1.12	–11.83
B1e	–6.05	–6.05	0.03	–12.07	0.59	–11.48
B1f	–6.04	–6.04	0.08	–12.00	0.61	–11.39
B1g	–5.95	–5.95	0.01	–11.89	0.55	–11.34
B1h	–6.14	–0.06	–3.76	–9.96	–0.22	–10.18

Figure 1. Molecular Electrostatic Potential (MEP) for the monomers: H_2CO, H_2CS and SO_2 at the MP2/aug-cc-pVDZ computational level. Upper and lower segments show the molecular plane, and a plane perpendicular to it, respectively. Red and blue regions indicate negative and positive zones, respectively of the ±0.032 au contour.

H_2CO	H_2CS	SO_2
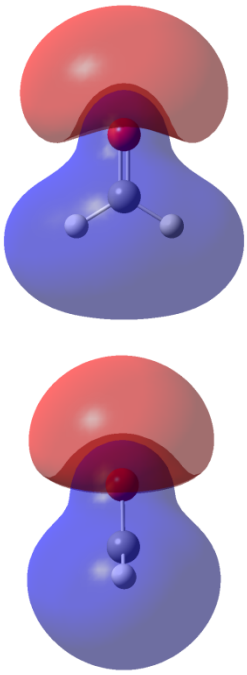	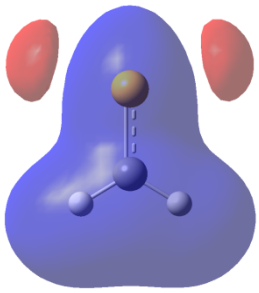	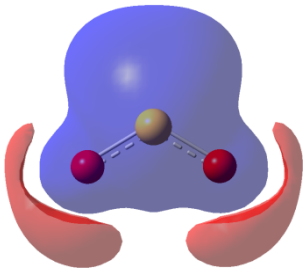
	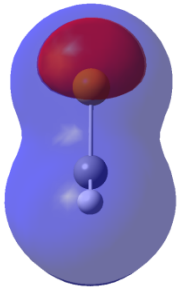	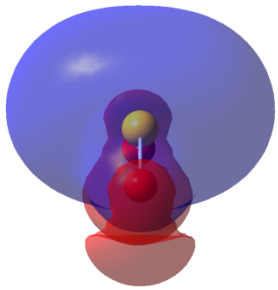

Figure 2. 1:1 complexes between SO_2 and H_2CX (X = O, S) at MP2/aug-cc-pVDZ computational level. Blue dot lines link atoms which present interatomic AIM BCPs, with interatomic distances in Å. Arrows indicate the direction of charge transfer. Complexes are arranged in ascending order of energy.

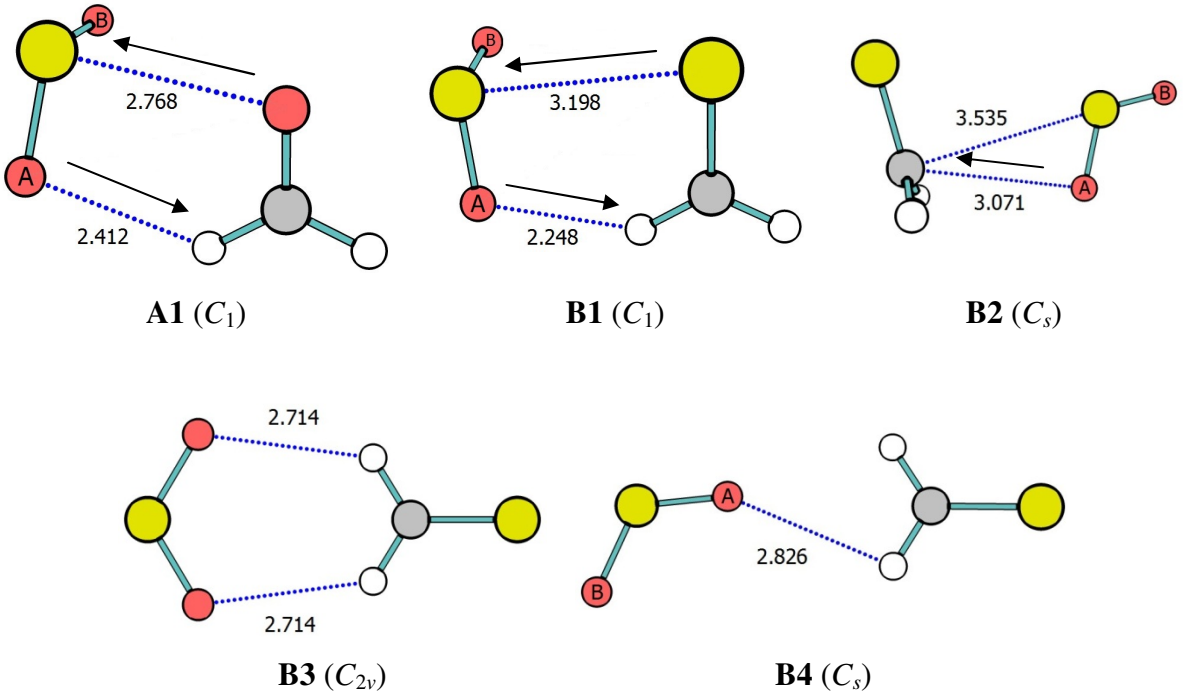

A1 (C_1) **B1** (C_1) **B2** (C_s)

B3 (C_{2v}) **B4** (C_s)

Figure 3. Electron Density Shifts (EDS) occurring in the 1:1 SO_2:H_2CX (X = O, S) complexes at MP2/aug-cc-pVDZ level. Purple and yellow refer to gain and loss of density in complex, respectively, relative to isolated monomers. Isosurface value ±0.001 au for **A1** and **B1**, and ±0.0005 au for **B2, B3** and **B4**.

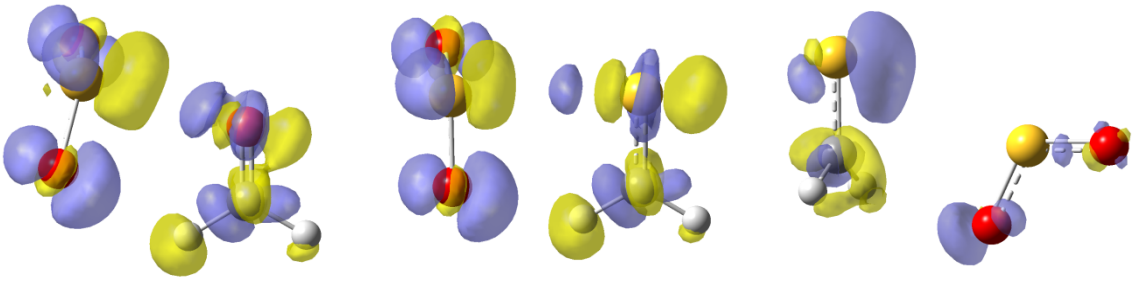

A1 (C_1) **B1** (C_1) **B2** (C_s)

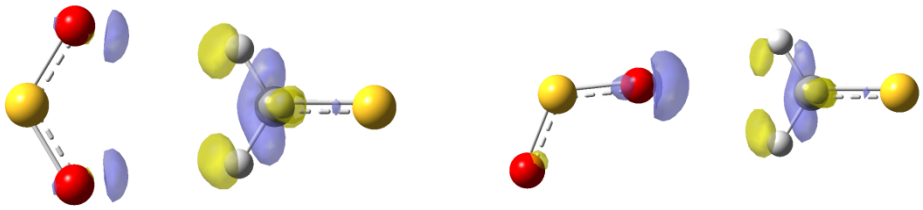

B3 (C_{2v}) **B4** (C_s)

Figure 4. 2:1 complexes between SO_2 and H_2CO derived from **A1** at MP2/aug-cc-pVDZ computational level. Broken lines link atoms which present interatomic BCPs, with interatomic distances in Å. Arrows indicate the direction of charge transfer. Complexes are arranged in ascending order of energy.

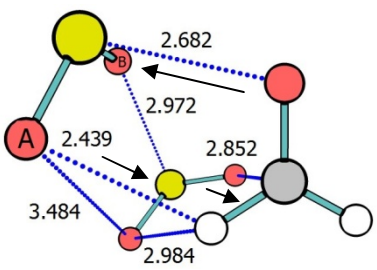

A1b (C_1)

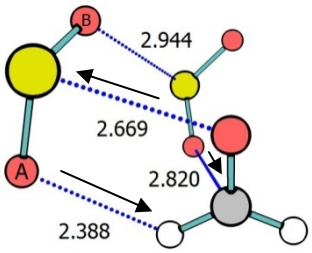

A1a (C_1)

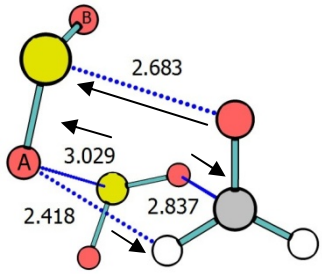

A1c (C_1)

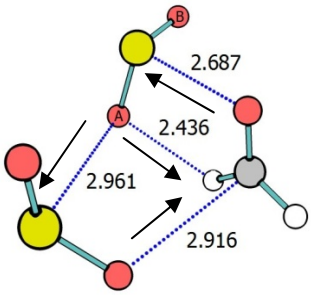

A1d (C_1)

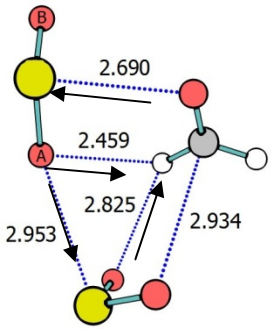

A1e (C_1)

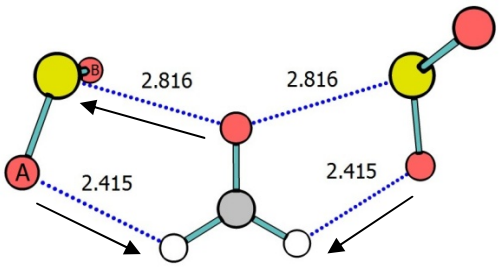

A1f (C_2)

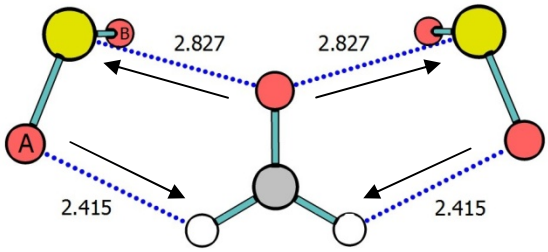

A1g (C_s)

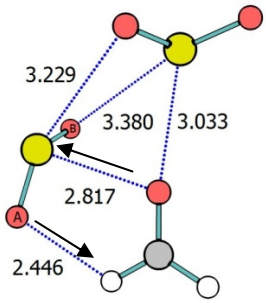

A1h (C_1)

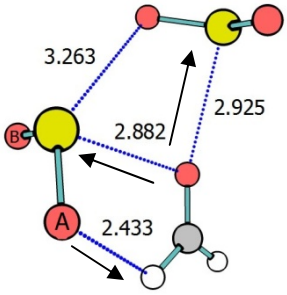

A1i (C_1)

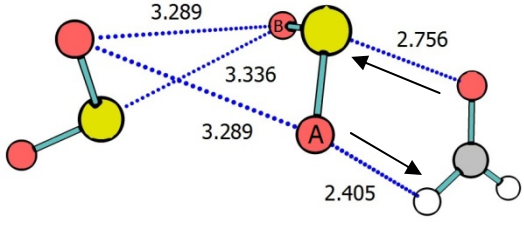

A1j (C_1)

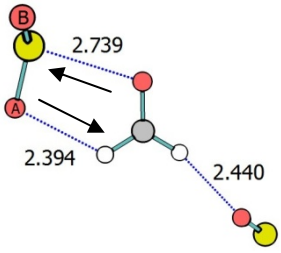

A1k (C_1)

Figure 5. 2:1 complexes between SO_2 and H_2CS derived from **B1** at MP2/aug-cc-pVDZ computational level. Broken lines link atoms which present interatomic BCPs, with interatomic distances in Å. Complexes are arranged in ascending order of energy.

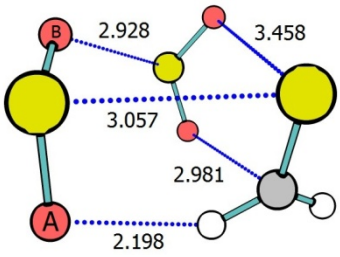

B1a (C_1)

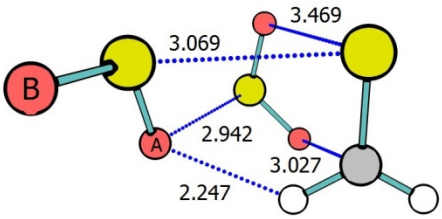

B1b (C_1)

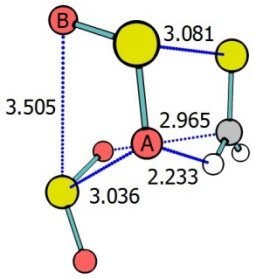

B1c (C_1)

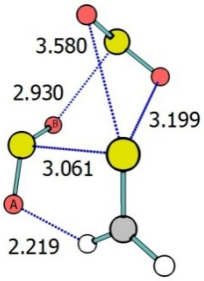

B1d (C_1)

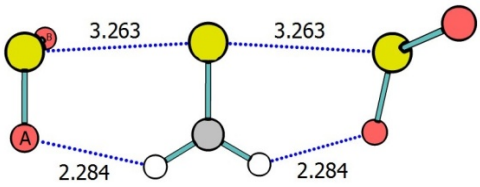

B1e (C_2)

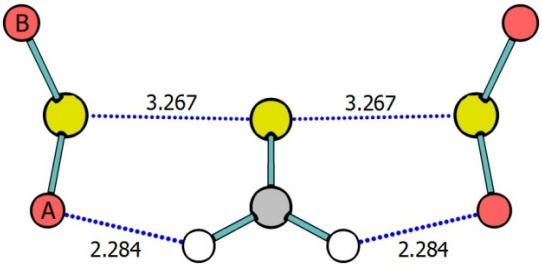

B1f (C_s)

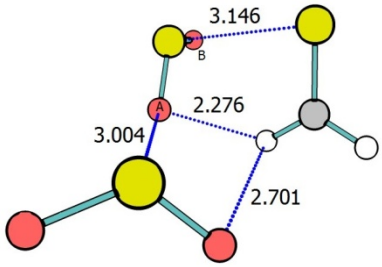

B1g (C_1)

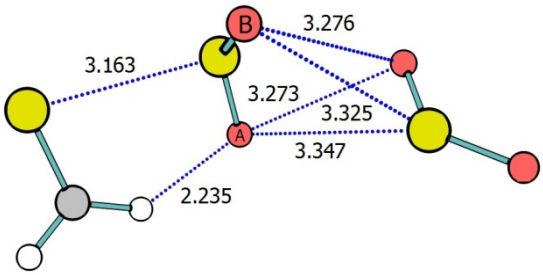

B1h (C_1)